JOURNAL OF SOLID STATE CHEMISTRY 71, 214–223 (1987)

Structural and Calorimetric Studies of Order–Disorder in $CdMg(CO_3)_2$

CHRISTOPHER CAPOBIANCO

Department of Earth Sciences, Cambridge University, Cambridge, England

BENJAMIN P. BURTON AND PAULA M. DAVIDSON

National Bureau of Standards, Gaithersburg, Maryland 20899

AND ALEXANDRA NAVROTSKY

Department of Geological and Geophysical Sciences, Princeton University, Princeton, New Jersey 08544

Received October 17, 1986; in revised form February 6, 1987

The disordering of $CdMg(CO_3)_2$ was studied near room temperature by powder X-ray diffraction and solution calorimetry using samples quenched from 600 to 850°C. The long-range order parameter changes from unity to zero in this range and the enthalpy of disordering is 13.7 ± 0.8 kJ/mole. The enthalpy of formation of ordered $CdMg(CO_3)_2$ from $CdCO_3$ and $MgCO_3$ is −5.6 ± 0.8 kJ/mole; that of the disordered phase is +8.1 ± 0.8 kJ/mole. These data support energetic models which assume positive interactions of Cd and Mg within cation layers and negative interactions (leading to ordering) between layers. A reasonable fit to the observed phase relations is achieved using either the point approximation (PA) of the generalized Bragg–Williams model or the tetrahedron approximation (TA) of the cluster variation method (CVM). These models however, do not give a quantitative fit to the variation of enthalpy and long-range order parameter with temperature. In particular, the observed order–disorder transition occurs more sharply over a smaller temperature range than predicted, perhaps because of more strongly cooperative behavior in which the carbonate groups as well as the divalent cations play a role.

Introduction

The calcite and dolomite crystal structures commonly occur in nature for divalent metal carbonate minerals (usually $CaCO_3$ and $CaMg(CO_3)_2$). The major crystal–chemical difference between the calcite and dolomite structures is that calcite contains only one distinct metal layer while dolomite has two (*1–4*). The chemical difference between these layers results in two geometrically inequivalent cation sites. Furthermore, a continuous range of possible structures between the ordered dolomite and disordered calcite structures is possible because the space group of dolomite ($R\bar{3}$) is a subgroup of that of calcite ($\bar{R}3c$). Indeed, some natural dolomites (i.e., $CaMg(CO_3)_2$) are reported to have disordered structural states (*4*) while synthetically disordered samples may be obtained by annealing ordered material at high tem-

0022-4596/87 $3.00

perature. However, the high temperatures involved and possible problems in quenching the disordered phase make detailed study of the order–disorder transition in $CaMg(CO_3)_2$ difficult.

The system $CdCO_3$–$MgCO_3$ offers an analog to the $CaCO_3$–$MgCO_3$ system in that similar ordered and disordered phases exist (*5*). Because chemical homogenization of distinct Cd and Mg layers proceeds within an experimentally accessible range of pressure and temperature (1–10 kbar pCO_2 and 600 to 850°C), samples can be prepared which, on quenching, possess greatly different states of order. In addition, the large difference in atomic number between Cd and Mg readily permits the study of the degree of long-range order by X-ray diffraction on powdered samples. The present study combines such structural work with a determination, by solution calorimetry, of the enthalpy associated with disordering and with the formation of the ordered compound from $CdCO_3$ and $MgCO_3$. The relationship between the structural state and disordering enthalpy is discussed in terms of models for the energetics of order–disorder reactions.

Experimental Methods

Synthesis and Characterization of Starting Material

The ordered compound $CdMg(CO_3)_2$ was synthesized from mulled endmember mixtures of $MgCO_3$ and $CdCO_3$ at 600°C under 1 kbar CO_2 pressure in a hydrothermal pressure vessel. Pure $MgCO_3$ was obtained by recrystallizing basic magnesium carbonate at 1 kbar CO_2 pressure and 600°C. Finely crystalline $CdCO_3$ was dried at 110°C and used without recrystallization for the synthesis runs. Both endmembers exhibited sharp calcite-type powder diffraction patterns and were found to be stoichiometric by weight loss after calcination. Synthesis runs lasting 4 days were sufficient to produce X-ray powder patterns with no detectable endmember diffraction peaks and intense ordering diffraction peaks indicative of the dolomite-type ordering. Anhedral crystals between 2 and 5 μm in diameter were obtained from nominally "dry" runs and no increase in grain size was apparent after an additional week of annealing. The bulk composition of the $CdMg(CO_3)_2$ was checked by EDTA titrations (*6*) on a split of the run product. The starting material was found to be stoichiometric at least to 0.1%.

Recrystallized $CdCO_3$ with grain sizes up to 10 μm was used for solution calorimetry required to determine the enthalpy of formation of $CdMg(CO_3)_2$.

Annealing Treatments

Samples of the highly ordered starting material synthesized as described above were subjected to annealing within the disordering interval of $CdMg(CO_3)_2$ reported by Goldsmith (*5*). A solid media piston cylinder pressure apparatus was necessary to achieve confining pressures sufficient to prevent loss of CO_2 from the carbonate between 750 and 850°C. Approximately 200 mg of sample was encapsulated in Pt and runs were monitored with W–Re thermocouples adjacent to the capsule. Conditions for the disordering runs are reported in Table I. Fairly rapid quench occurred in the solid media pressure apparatus with tem-

TABLE I

PISTON CYLINDER SYNTHESES OF $CdMg(CO_3)_2$

mg Sample	T (°C)	P (kbar)	t (hr)	a_{rh} (Å)	α (deg)
223	750	10	2	5.8931(29)	47.747(29)
145	775	15	1.5	5.9065(90)	47.662(10)
239	850	15	3	5.9020(11)	47.660(13)
750	600	1[a]	168	5.8931(10)	47.781(11)

[a] Hydrothermal pressure vessel using CO_2 fluid pressure.

peratures falling from run conditions to 400°C within 1 or 2 sec. Greatly reduced peak intensities for the ordering diffraction peaks indicated that long-range order destroyed at run conditions was not regained during quench.

X-Ray Diffraction Measurements

The lattice parameters of the starting material and annealed calorimetric samples were obtained from X-ray powder diffraction data using Guinier camera techniques and an internal standard of NBS Si No. 640. Results of least-squares refinements using at least 10 diffraction line positions are reported in Table I.

Intensity data for the ordering reflections were obtained from the average areas of three diffractometer scans over the diffraction peaks using Cu$K\alpha$ radiation. Since the run products generally showed no grain growth (except for highly disordered 850°C sample) and crystals were anhedral, there should be no preferred orientation effects inherent in the intensity data. Table II reports the intensity ratios of the ordering reflections obtained by normalizing peak areas of annealed samples to corresponding peaks in the ordered starting material.

Calorimetric Techniques

After preliminary experiments with several aqueous and molten salt solvents at 80–350°C, an aqueous solvent saturated in NaCl and containing 1.0 *M* HCl, 0.75 *M* $CaCl_2$, 0.25 *M* $MgCl_2$ at room temperature was adopted. The high ionic strength acid brine has a low vapor pressure and low CO_2 solubility and rapidly dissolves carbonates reproducibly at 85°C. Heats of solution were obtained in this solvent using a Tian-Calvet heat flow calorimeter operating at 85°C. The experimental arrangement is shown in Fig. 1.

Prior to dissolution, samples were encapsulated in thin-walled Pyrex tubes to pre-

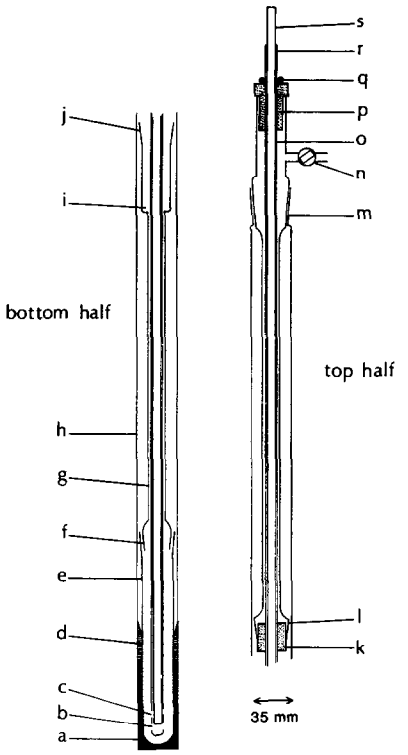

FIG. 1. Calorimetric apparatus: a, exterior aluminum crucible; b, ports in manipulation assembly to hold sample capsule; c, venting ports in sample manipulation assembly; d, Kovar glass-to-metal seal; e, Pyrec reaction crucible; f, ground-glass joint (24/25); g, Pyrex containment vessel; h, Pyrex liner (35 mm o.d.); i, condensation reservoir; j, ground-glass joint, female (24/25); k, Teflon manipulation assembly stabilizer; l, ground-glass joint, male (24/25); m, ground-glass joint (34/28); n, stopcock, outlet to bubbler; o, sample manipulation tube (10 mm); p, Teflon sample manipulation assembly holder; q, O-ring; r, vacuum grease; s, sample manipulation rod to crush capsule.

TABLE II

X-RAY INTENSITY RATIOS OF DOLOMITE-TYPE REFLECTIONS (NORMALIZED TO 600°C INTENSITIES)

$(hkl)_m$	750°C	775°C	850°C
111	0.388(43)	0.331(32)	0.0
100	0.422(36)	0.352(30)	0.038(5)
221	0.426(33)	0.379(14)	0.004(4)
322	0.490(50)	0.416(24)	0.0
111	0.424(28)	0.436(23)	0.0

vent prereaction of the samples with the corrosive solvent. Runs were initiated after thermal equilibrium was attained in the calorimeter by crushing the Pyrex sample tube. The dissolution was completed within 30 sec but the resulting calorimetric peak lasted between 1 and 2 hr because of the long time constant of the large-volume calorimeter used. The total heat effect measured was about 4 joules. Further details of the experimental method are found in Capobianco (*7*). An advantage of this calorimetric solvent is the relatively small magnitude (<30 kJ/mole) of the experimental heats of solution. A potential disadvantage is the complexity of ionic interactions in this multicomponent hot aqueous solution, to which the laws of dilute solution may not apply. To permit unequivocal interpretation of the enthalpies of solution several precautions were taken: (1) The excess enthalpy of partially disordered samples was found by the difference in heats of solution between the disordered samples and the fully ordered 600°C sample. (2) The volume of solvent and the mass of all samples dissolved was held strictly constant for all runs (40.0-mg samples were dissolved in 10.0 ml solvent). This procedure made it unnecessary to correct for the work done in CO_2 evolution or to unravel the complex chemical interactions within the solvent.

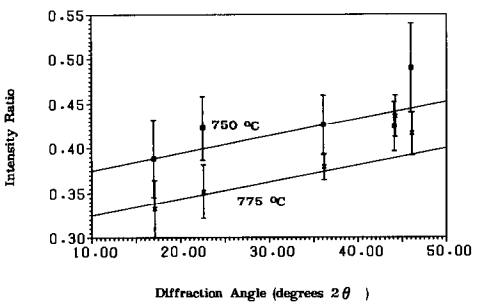

FIG. 2. Experimental ratio of intensities of ordering peaks for partially disordered versus fully ordered diffraction peaks versus diffraction angle for samples quenched from 750 and 775°C.

The difference in enthalpy of solution of ordered and partially disordered samples then directly gave the excess enthalpy stored in the latter. The enthalpy of formation from $CdCO_3$ and $MgCO_3$ of stoichiometric Cd-dolomite was obtained as the difference of the heats of solution of a stoichiometric mechanical mixture of end member carbonates and of the compound.

Results

Long-Range Order Parameters for Partially Disordered Cd-Dolomites

Normalization of the X-ray intensity data by the corresponding reflection intensity of the fully ordered starting material eliminates variations between different reflections associated with differences in reflection multiplicity or $\sin(\theta)/\lambda$ effects. The square of the ratio of structure factors for the ordering reflections (i.e., $h + k + l$ odd and two or three rhombohedral indices alike) may then be compared with the experimental data (Table II) to assess the long-range order between cation layers. Graf (*8*) provides the appropriate structure factor equation for dolomite-type reflections in the rhombohedral description:

$$F_{hkl} = f_{Cd} - f_{Mg} + f_C\cos[2\pi(h + k + l)x_C] + f_O\cos[2\pi(hx_O + ky_O + lz_O)] + \cos[2\pi(lx_O + hy_O + kz_O)] + \cos[2\pi(kx_O + ly_O + hz_O)] \quad (1)$$

Because the difference in atomic scattering factors between Cd and Mg ($f_{Cd} - f_{Mg}$) is large, the dolomite-type reflections for this material are intense and contain a dominant intensity contribution from the cation sublattice. Moreover, the cation sublattice contribution does not vary among the several ordering reflections. Any observed variation of the intensity ratios is, therefore, the effect of the carbonate sublattice. Figure 2 shows the experimental intensity ratios versus the diffraction angle for the

750 and 775°C samples. Although the measured variation is slight, the experimental errors are not sufficiently great to obscure the *hkl* dependence.

The carbonate sublattice differs slightly between calcite and dolomite structures in the Ca–Mg system, but there are no single-crystal refinements of the $CdMg(CO_3)_2$ phases to provide the precise details. Thus, it is necessary to estimate carbonate positional parameters (x_C, x_O, y_O, z_O) for the fully ordered material and to model their variation as a function of cation order.

The calcite phase has only one variable positional parameter (an oxygen parameter) which may be easily approximated by assuming a fixed C–O bond length for the carbonate (1.285 Å) (*9*). In the calcite structure the carbon location is fixed by its *ccp*-type alternation with identical cation nets and the C–O bond lies directly along the a_{hex} unit cell vector. The free parameter for oxygen is then determined by the ratio of the C–O bond length to the a_{hex} unit cell length.

In the dolomite structure the situation is slightly more complex. The carbon shifts its location along c_{hex}, presumably in response to unequal interactions with chemically distinct cation layers, while the C–O bond shifts away from the a_{hex} direction, creating two unequal metal–oxygen distances. Unlike the case for calcite, the crystallographic coordinates for the oxygen (now in a general position) cannot be fixed using constant carbon–oxygen bond lengths and crystal geometry because the carbon location is no longer constrained to be equidistant between metal layers. Furthermore, the carbonate units in dolomite-type crystals need not be strictly planar. Beran and Zemann (*9*), among others, report slightly tetrahedral carbonate groups in $CaMg(CO_3)_2$. We use the crystal coordinates of the carbonate from the isostructural $CaMg(CO_3)_2$ (*4*, *9*) as reasonable estimates for its location in Cd-dolomite. The error introduced by this approximation does not significantly alter the calculated long-range order for the cation sublattice.

To incorporate the effect of disorder, one may replace the atomic scattering factors for the Cd and Mg sites (f_{Cd} and f_{Mg}) in Eq. (1) by effective scattering factors containing contributions from both atoms:

$$f_{Cd}^{eff} = x f_{Cd} + (1 - x) f_{Mg}$$
$$f_{Mg}^{eff} = (1 - x) f_{Cd} + x f_{Mg} \qquad (2)$$

In these equations x represents the fractional occupancy of the cation sites by the "right" atom and may vary between 0.5 and 1. The long-range cation order parameter is then obtained from x by

$$s = 2x - 1, \qquad (3)$$

where s can take on values between zero for a disordered calcite-like phase and unity for a fully ordered dolomite phase. The trigonometric arguments of Eq. (1) are given a simple s dependence such that the carbonate positional parameters correspond to fully ordered Cd-dolomite at $s = 1$ and totally disordered $CdMg(CO_3)$ at $s = 0$.

The true functional dependence of the average carbonate position on s would give information about the relative rates of structural change for the cation and anion sublattices. However, for lack of data, we assign only a simple linear dependence for intermediate carbonate positional parameters, $x_i(s)$:

$$x_i(s) = x_i^{dis} + s(x_i^{ord} - x_i^{dis}). \qquad (4)$$

For each observed reflection one may then construct ratios of the structure factor equations to be compared with experimental data:

$$I_{hkl}^{dis}/I_{hkl}^{ord} = (F_{hkl}^{(s)}/F_{hkl}^{(1)})^2. \qquad (5)$$

Average values for s obtained from Eq. (5) are given in Table III for the 750, 775, and 850°C samples. The quoted errors are the standard deviations from the averages based on the five reflections for each sample. The results confirm Goldsmith's ear-

TABLE III

CALORIMETRIC DATA, ORDER PARAMETERS, AND ENTHALPIES OF DISORDERING AND MIXING

T (°C)	Order parameter, s[a]	Enthalpy (kJ/mole $CdMg(CO_3)_2$ Solution[b]	Disordering[c]	Mixing[d]
600	1	33.87 ± 0.23	0	−5.63 ± 0.8
750	0.656 ± 0.036	27.36 ± 0.29	6.51 ± 0.4	+0.88 ± 0.8
775	0.620 ± 0.028	27.19 ± 0.30	6.68 ± 0.4	+1.05 ± 0.8
850	0.052 ± 0.078	20.12 ± 0.49	13.75 ± 0.8	+8.12 ± 0.8
—	—	28.24 ± 0.48[e]	—	—

[a] Calculated as described in text. Error is standard deviation based on the five reflections used.

[b] From calorimetry error is standard deviation of mean.

[c] For reaction $CdMg(CO_3)_2$ (ordered) = $CdMg(CO_3)_2$ (partially or totally disordered), from difference in enthalpy of solution of two samples. Error from propagation of errors in heats of solution.

[d] For reaction $CdCO_3 + MgCO_3 = CdMg(CO_3)_2$, from difference in enthalpy of solution of sample and mechanical mixture. Error from propagation of errors in enthalpies of solution.

[e] Mechanical mixture.

lier, more qualitative work (*5*). Samples prepared at 600°C are fully ordered, those at 850°C are virtually completely disordered (our long-range order parameter is zero within experimental error), while those quenched from intermediate temperatures, 750 and 775°C, show values of s between 0.6 and 0.7.

Enthalpies of $CdMg(CO_3)_2$ of Different Degrees of Order

The calorimetric data are summarized in Table III. For the formation of the ordered dolomite from the endmember carbonates

$$CdCO_3 + MgCO_3 = CdMg(CO_3)_2 \text{ (ordered)}$$
$$\Delta H^0 = -5.6 \pm 0.8 \text{ kJ/mole}, \quad (6)$$

confirming the energetic stability of the ordered compound. However, the heat of mixing in the disordered solid solution is positive; i.e., for the reaction

$$CdCO_3 + MgCO_3 = CdMg(CO_3)_2 \text{ (disordered solid solution)},$$
$$\Delta H^0 = +8.1 \pm 0.8 \text{ kJ/mole}. \quad (7)$$

Both calorimetric and X-ray measurements were made near room temperature on samples quenched from 600 to 800°C. Two factors may potentially complicate the application of these measurements to high-temperature equilibria. One would be any change in short- or long-range order during quench. As mentioned above, quench rates were fairly rapid, the temperature falling to 400°C in 1–2 sec. Both this work and previous studies of Goldsmith (*5*) suggest that changes in long-range order appear to be reversible on a time scale of hours and quenchable on a time scale of seconds. Little can be said about short-range order. The second effect which might modify the thermodynamics is any strong temperature dependence in the enthalpy of disordering resulting from a substantial difference in vibrational heat capacity between ordered and disordered phases. Though no such C_p data exist for these carbonates, it is unlikely that any such effect gives a correction term as large as the uncertainty (±0.8 kJ/mole) in the measured enthalpy of disordering. With these points in mind, the data obtained for $CdMg(CO_3)_2$ by measurements near room temperature can be applied to model this disordering equilibria at 600–800°C.

Discussion of Models for the Order–Disorder Reaction

Bragg–Williams Approximation

The Cd, Mg disordering reaction is convergent (*10*); i.e., alternate cation layers are crystallographically distinct only when the cations are ordered. The simplest model which can be applied to the order–disorder reaction is of the Bragg–Williams types (*11–13*), in which the long-range order parameter s is related to one energy parameter, W, by the equations (at the stoichiometric dolomite composition):

$$s = \tanh(-Ws/2R), \quad (8)$$

where W is negative and its numerical value reflects the energy per mole of $CdMg(CO_3)_2$.

The enthalpy of mixing (formation of $CdMg(CO_3)_2$ from $CdCO_3$ and $MgCO_3$) is then

$$\Delta H^{mix} = W[0.5 - 0.25(1 - s^2)]$$
$$0.5W \leq \Delta H^{mix} \leq 0.25W. \quad (9)$$

The critical temperature at which s becomes zero is given by $T_c = -W/2R$. The X-ray diffraction data above imply that T_c is near 1123 K (850°C) and $W = -2RT_c = -18.7$ kJ mole. Using this value, the values of order parameter and enthalpy at lower temperatures are not described well. Increasing the magnitude of W would improve the fit to the order parameter at lower temperature but would erroneously predict the persistence of long-range order above 850°C.

However, the Bragg–Williams approximation has an even more serious qualitative shortcoming. It cannot account for positive enthalpies of mixing in the disordered solid solution because its one parameter, W, must be negative for ordering to take place at low temperatures. Thus (see Eq. (9)), even the disordered phase would show a negative heat of mixing.

Generalized Point Approximation

To include positive heats of mixing in the disordered phase, one can apply a generalized Bragg–Williams, or generalized point approximation (PA) (*14, 15*), in which there are two distinct interactions: (1) an attractive (interlayer) interaction promoting unlike pair formation (parameterized as W_{ier}) and a repulsive (intralayer) interaction promoting segregation (parameterized as W_{ira}).

The Gibbs free energy of mixing (formation of $(Cd_{1-x}Mg_x)_2(CO_3)_2$ from $CdCO_3$ and $MgCO_3$) is given by, per formula unit containing two carbonates,

$$\Delta G^{mix} =$$
$$W_{ier}[x - x^2(1 - s^2)] + W_{ira}[x - x^2(1 + s^2)]$$
$$+ RT \sum_i \sum_j x_{ij} \ln x_{ij}, \quad (10)$$

where x_{ij} is the cation site occupancy of the jth atom on the ith sublattice. Thus for $i = \alpha$ (layer preferred by Mg), β (layer preferred by Cd) and j = Mg, Cd, $x_{\alpha,Mg} = x + xs$, $x_{\alpha,Cd} = 1 - x - xs$, $x_{\beta,Mg} = x - xs$, and $x_{\beta,Cd} = 1 - x + sx$. Here x is the mole fraction of $MgCO_3$ ($0 < x < 1$) and s, as before, is the long-range order parameter ($0 \leq x \leq 1$ for $x \leq 0.5$ and $0 \leq s \leq (1/x - 1)$ for $x \geq 0.5$). As in the original Bragg–Williams model, the equilibrium value of s is found by minimizing ΔG^{mix} with respect to variations in s, and the critical temperature for disordering is obtained by setting the second derivative of ΔG^{mix} to zero for $s = 0$. For $W_{ier} < 0$ and $W_{ira} > 0$, intersite ordering decreases ΔH^{mix} while intrasite mixing increases it, and at low temperature the ordered phase is stable. Above T_c, $s = 0$, so that ΔH^{mix}, given by $(W_{ier} + W_{ira})(x - x^2)$ is positive for $W_{ira} > |W_{ier}|$. W_{ier} and/or W_{ira} may depend on composition, leading to asymmetry in solution properties. Phase relations in the join $(Cd, Mg)CO_3$ were found by Goldsmith (*5*) to be asymmetric; see Fig. 4. This indicates that at least one additional parameter is required to fit both the thermochemical and phase equilibrium data. We chose to replace W_{ira} by $A + Bx$ to introduce the required asymmetry. The parameters W_{ier}, A, and B were then optimized with respect to the enthalpy of solution measurements and phase equilibrium data by a nonlinear least-squares technique. Because it was not possible to simultaneously satisfy the two sources of data, two different parameter sets were obtained. PA_1 was fit to phase equilibrium data only. PA_2 was developed in two stages: first, W_{ier} and W_{ira} were optimized with respect to ΔH^{mix}, at $x = 0.5$; then B/A was optimized with respect to the phase equilibrium data, at $A + 0.5B$ = constant. The parameters used (kJ per mole of $(Cd_xMg_{1-x})_2(CO_3)_2$) were $PA_1(A = -8.5, B = 16 + 30.9x)$ and $PA_2(A = -13.3, B = -0.425 + 47.5x)$. The calculated results are shown in Figs. 3 and 4.

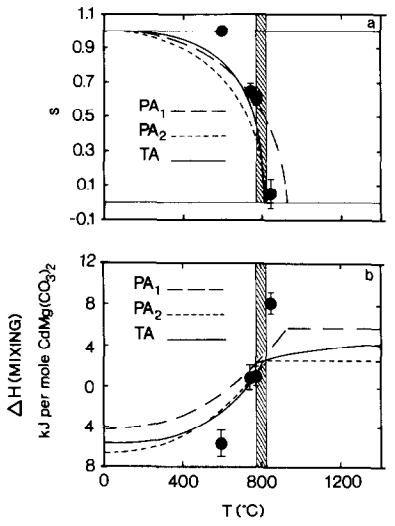

FIG. 3. (a) The long-range order parameter s as a function of temperature. PA_1 and PA_2, generalized point approximations 1 and 2, respectively: TA, tetrahedron approximation. (b) Mixing enthalpy (for the reaction $CdCO_3 + MgCO_3 = MgCd(CO_3)_2$) as a function of temperature calculated from the above models. In both a and b experimental values for Table III are shown as points with error bars. Hatched areas indicate range in T_c.

Tetrahedron Approximation in the Cluster Variation Method

A third model, based on the tetrahedron approximation (TA) in the cluster variation method (CVM) was also considered. The formalism has been described previously (*16*, *17*), so only details pertaining to $CdCO_3$–$MgCO_3$ are given here. The CVM approach attempts to include the effects of short-range order (which the point or Bragg–Williams approximations neglect) by considering the possible arrangements of clusters of atoms (cation tetrahedra in this case). The calculated equilibrium proportions of the chemically distinct tetrahedra are constrained by the total solution composition and the energetic interactions between the atoms of the tetrahedron. These calculated proportions then provide information on both long-range and short-range order. Because of short-range order, the configurational entropy in the CVM calculations is generally smaller than in the previous models.

For the $CdCO_3$–$MgCO_3$ calculations, a three-parameter version of the TA was used in order to account for the observed asymmetry in the phase relations. The pairwise interaction parameters ε_{ier}, and $\varepsilon_{ira} = A + (N_{Mg} - N_{Cd})B$, have essentially the same meaning as W_{ier} and W_{ira}, respectively (N_{Mg} and N_{Cd} are the numbers of Mg and Cd atoms in a tetrahedral cluster; see (*16*, *17*) for a detailed discussion). The values of ε_{ier}, A, and B that were used in model TA ($\varepsilon_{ier} - 0.938$, $A = 3.003$, and $B = 1.595$ kJ/mole), were constrained to yield $\Delta H^{mix} = -5.63$ kJ/mole $CdMg(CO_3)_2$, $775° < T_c < 825°C$ (*4*), and $T_{cons}/T_c = 1.05(5)$ where T_{cons} is the consolute temperature for two disordered phases. The TA is therefore most closely comparable to PA_2 because it was fit to both thermochemical and phase equilibrium data. However, its parameters were not optimized by a least-squares technique.

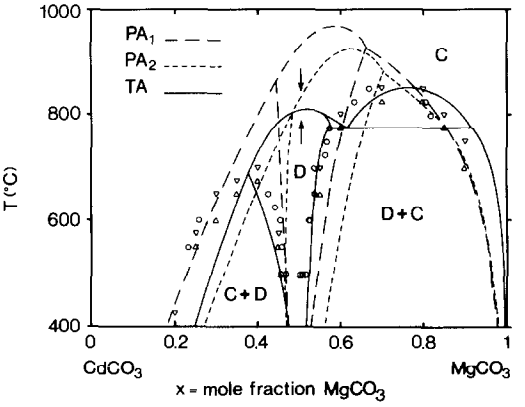

FIG. 4. Comparison of the experimental phase equilibrium data (*4*) with the model calculations PA_1, PA_2, and TA. C, a disordered calcite phase with calcite structure, space group $R\bar{3}c$; D, ordered phase with dolomite structure, space group $R\bar{3}$. Triangles correspond to large open circles in (*5*), and circles correspond to filled circles in Goldsmith (*5*). ↑, The experimental lower limit $T_c > 775°C$, this work; ↓, the experimental upper limit $T_c \leq 825°C$ (*5*).

Comparison of Models with Experiment

Figure 3 shows the calculated long-range order parameter s and enthalpy of mixing as functions of temperature. The experimental data are also shown. Figure 4 compares calculated and experimental phase diagrams. None of the models discussed here achieves quantitative agreement with both the thermochemical and the phase equilibrium data, but certain interesting trends are evident. With regard to the order–disorder transition in $CdMg(CO_3)_2$, all three models underestimate the sharpness of transition in the sense that experimental values of ΔH^{mix} and s change much more rapidly with temperature than the models predict. The calculations also underestimate the magnitude of the positive enthalpy of mixing seen in the long-range disordered phase. Although the TA predicts a somewhat sharper transition than PA_1 or PA_2 (Figs. 3a and 3b), it is still very far from a quantitative fit to the calorimetric values. It appears unlikely that a higher order CVM approximation would yield the kind of dramatic improvement that is needed for a quantitative fit. The comparison between experimental phase equilibria and the calculated phase diagrams is more compelling. The generalized point approximation (PA_1 and PA_2) can generate phase diagrams with a stability field for two disordered phases, but in these diagrams the tricritical point at the crest of the Cd-rich two-phase field (C + D, Fig. 4) occurs at temperatures that are much too low. Thus, the TA appears to give a more realistic fit to the combined thermochemical plus phase equilibria data set.

The failure of the above models to predict energetics quantitatively may be related to several factors. First, the carbonate group may undergo shifts of position and small deviations from a planar configuration as a result of Cd, Mg ordering. Such involvement of CO_3 groups might give the transition more cooperative character and compress it, as observed, into a smaller temperature interval. Second, the compositional asymmetry of inter- and intralayer interactions may be more complex than considered here. Third, differences in lattice vibrations between ordered and disordered phases may result in excess heat capacities, excess entropies, and temperature-dependent enthalpies not considered in simple models.

Despite the above complexities, we conclude that relatively simple statistical models can qualitatively explain the variation of long-range order with temperature, the enthalpy of mixing, and the topology of the phase diagram. Such models incorporate three main features: a negative (stabilizing) interaction for ordering of Cd and Mg between layers, a positive (destabilizing) interaction for the mixing of Cd and Mg within a layer, and compositional asymmetry for at least one parameter. Similar arguments hold for the $MgCO_3$–$CaCO_3$ system (*16, 17*), though complete thermochemical data for disordering are not available.

Acknowledgments

This work was supported by National Science Foundation Grants DMR 8106027 and 8521562 from the Solid State Chemistry Program.

References

1. W. H. Bragg and W. L. Bragg, "X Rays and Crystal Structure." Bell, London (1915).
2. J. A. Wasastjerna, *Soc. Sci. Fennica Commun. Phys. Math.* **2,** 1 (1924).
3. R. W. G. Wyckoff and H. K. Merwin, *Amer. J. Sci.* **8,** 447 (1924).
4. R. J. Reeder, *in* "Reviews in Mineralogy," Vol. 11, "Carbonates" (R. J. Reeder, Ed.), p. 1. Mineral. Soc. Amer., Washington, DC (1983).
5. J. R. Goldsmith, *J. Geol.* **80,** 617 (1972).
6. H. Flaschka, *Chem. Anal.* **41,** 50 (1953).
7. C. Capobianco, "Thermodynamic Relations of

Several Carbonate Solid Solutions," Ph.D. thesis. Arizona State Univ. (May 1986).
8. D. L. GRAF, *Amer. Mineral.* **46,** 1283 (1961).
9. A. BERAN AND J. ZEMANN, *Tschermak's Mineral. Petrog. Mitteil.* **24,** 279 (1977).
10. J. B. THOMPSON, *Amer. Mineral.* **54,** 341 (1969).
11. W. F. BRAGG AND E. J. WILLIAMS, *Proc. R. Soc. London Ser. A* **145,** 699 (1934).
12. A. NAVROTSKY AND D. LOUCKS, *Phys. Chem. Mineral.* **1,** 109 (1977).
13. B. A. WECHSLER AND A. NAVROTSKY, *J. Solid State Chem.* **55,** 165 (1984).
14. G. INDEN, *Acta Metall.* **22,** 945 (1974).
15. B. P. BURTON AND P. M. DAVIDSON, *in* "Advances in Physical Geochemistry," in preparation.
16. B. P. BURTON, *Amer. Mineral.* **72,** 329 (1987).
17. B. P. BURTON AND R. KIKUCHI, *Amer. Mineral.* **69,** 165 (1984).